Journal of Biotechnology 157 (2012) 326–333

Contents lists available at SciVerse ScienceDirect

Journal of Biotechnology

journal homepage: www.elsevier.com/locate/jbiotec

A rapid, targeted, neuron-selective, *in vivo* knockdown following a single intracerebroventricular injection of a novel chemically modified siRNA in the adult rat brain

Hidemitsu Nakajima[a,*,1], Takeya Kubo[a,1], Yuko Semi[a], Masanori Itakura[a], Mitsuru Kuwamura[b], Takeshi Izawa[b], Yasu-Taka Azuma[a], Tadayoshi Takeuchi[a]

[a] *Laboratory of Veterinary Pharmacology, Graduate School of Life and Environmental Sciences, Osaka Prefecture University, 1-58, Rinkuourai-kita, Izumisano, Osaka 5988531, Japan*
[b] *Laboratory of Veterinary Pathology, Graduate School of Life and Environmental Sciences, Osaka Prefecture University, 1-58, Rinkuourai-kita, Izumisano, Osaka 5988531, Japan*

ARTICLE INFO

Article history:
Received 5 July 2011
Received in revised form
30 September 2011
Accepted 5 October 2011
Available online 6 November 2011

Keywords:
RNA interference
Accell siRNA
In vivo delivery
Rat brain
Cyclophilin-B
GAPDH

ABSTRACT

There has been a dramatic expansion of the literature on RNA interference and with it, increasing interest in the potential clinical utility of targeted inhibition of gene expression and associated protein knockdown. However, a critical factor limiting the experimental and therapeutic application of RNA interference is the ability to deliver small interfering RNAs (siRNAs), particularly in the central nervous system, without complications such as toxicity and inflammation. Here we show that a single intracerebroventricular injection of Accell siRNA, a new type of naked siRNA that has been modified chemically to allow for delivery in the absence of transfection reagents, even into differentiated cells such mature neurons, leads to neuron-specific protein knockdown in the adult rat brain. Following *in vivo* delivery, targeted Accell siRNAs were incorporated successfully into various types of mature neurons, but not glia, for 1 week in diverse brain regions (cortex, striatum, hippocampus, midbrain, and cerebellum) with an efficacy of delivery of approximately 97%. Immunohistochemical and Western blotting analyses revealed widespread, targeted inhibition of the expression of two well-known reference proteins, cyclophilin-B (38–68% knockdown) and glyceraldehyde 3-phosphate dehydrogenase (23–34% knockdown). These findings suggest that this novel procedure is likely to be useful in experimental investigations of neuropathophysiological mechanisms.

Published by Elsevier B.V.

1. Introduction

Gene silencing by RNA interference has emerged as a promising new method of inhibiting the expression of targeted genes and inducing knockdown of associated proteins both *in vitro* and *in vivo* (Akhtar and Benter, 2007; de Fougerolles et al., 2007; Elbashir et al., 2001; Shim and Kwon, 2010). RNA interference has been applied in experimental investigations of physiological and pathophysiological mechanisms in animal models, and also has been considered as a potential clinical tool in the treatment of intractable illnesses including cancer, infectious diseases, and neurodegenerative and neuropsychiatric disorders (Akhtar and Benter, 2007; Chen and Zhaori, 2011). Thus, findings from studies involving *in vivo* application of small interfering RNAs (siRNAs) in animal models may be useful in inspiring clinical studies and predicting unintended off-target effects and adverse reactions such as recruitment of immune responses (Akhtar and Benter, 2007; Chen and Zhaori, 2011).

Unfortunately, naked siRNAs generally are not stable enough to exert their expected effects *in vivo* because they are degraded rapidly by endo- and exonucleases (Shim and Kwon, 2010). Various delivery systems have been developed to circumvent this problem, including liposomes (Zimmermann et al., 2006), cationic polymers (Pulford et al., 2010), viruses (Dreyer, 2011), chemical modifications (Walton et al., 2010), short peptide-conjugations (Kumar et al., 2007), electroporation (Zhao et al., 2005), and exosomes (Alvarez-Erviti et al., 2011). In the central nervous system (CNS), topical injection of naked siRNAs has been used successfully to induce gene silencing, although the efficacy of siRNA delivery is adequate only immediately surrounding the injection site and not

Abbreviations: siRNA, small interfering RNA; i.c.v., intracerebraventricular or intracerebraventricularly; CNS, central nervous system; FAM, carboxyfluorescene; DAPI, 4′,6-diamidino-2-phenylindole; DAB, 3,3-diaminobenzidine; GFAP, glial fibrillary acidic protein; Iba-1, ionized calcium binding adaptor molecule-1; CNP, 2′3′ cyclic nucleotide 3′ phosphodiesterase antibody; GAPDH, glyceraldehydes-3-phosphate dehydrogenase; IF, immunofluorescence.

* Corresponding author. Tel.: +81 72 463 5264, fax: +81 72 463 5264.
E-mail address: hnakajima@vet.osakafu-u.ac.jp (H. Nakajima).

[1] These authors equally contributed to this study.

0168-1656/$ – see front matter. Published by Elsevier B.V.
doi:10.1016/j.jbiotec.2011.10.003

at more remote locations (Jean et al., 2007; Lingor et al., 2005; Makimura et al., 2002; Manrique et al., 2009). Intracerebroventricular (i.c.v.) injection of siRNAs conjugated to a lipid-based reagent (e.g., Lipofectamine 2000) has also shown promise, but this approach may possibly raise concerns about toxicity and recruitment of immune responses induced by the lipid-based reagent (Chen et al., 2009; Hu et al., 2009; Thakker et al., 2004, 2005).

Thermo Scientific Dharmacon Accell siRNA is a new type of naked siRNA that has been modified chemically to allow for delivery without requiring transfection reagents, resulting in robust silencing of selected genes and knockdown of associated proteins. Accell siRNA is designed to minimize off-target effects, toxicity, and recruitment of immune responses (Baskin et al., 2008). To date, there have been several studies in which Accell siRNA has been used successfully to induce robust gene silencing and knockdown of targeted genes and proteins in neurons, but these have been exclusively *in vitro* cell culture studies (Dolga et al., 2008; Dreses-Werringloer et al., 2008; Sebeo et al., 2009; Suzuki et al., 2010). A few reports have appeared in which Accell siRNA was delivered *in vivo* via intravenous and nasal routes (Bonifazi et al., 2010; Difeo et al., 2009), but none of these studies involved delivery into the adult brain.

In the present study we demonstrate that rapid, targeted, neuron-selective, *in vivo* knockdown can be achieved in the adult rat brain following a single i.c.v. injection of Accell siRNA. This novel methodology has considerable potential utility as an experimental tool.

2. Materials and methods

2.1. Materials

Chemicals: Unless otherwise noted, reagents were of analytical grade.

Accell siRNA: The sequences of the siRNAs were as follows:

Accell carboxyfluroescence (FAM)-labeled control siRNA and Accell control siRNA, 5′-UGGUUUACAUGUCGACUAA-3′; Accell rat cyclophilin-B siRNA, 5′-CCUUUGGACUCUUUGGAAA-3′; Accell rat glyceraldehyde 3-phosphate dehydrogenase (GAPDH) siRNA, 5′-UCUACAUGUUCCAGUAUGA-3′.

2.2. A single i.c.v. injection of Accell siRNA

The experiments were performed in accordance with the guidelines of the Animal Ethical Committee of Osaka Prefecture University. Male Wistar rats (SLC Japan, Shizuoka, Japan) weighing 250–350 g were anesthetized with pentobarbital (50 mg/kg, i.p., Abbott Japan, Tokyo, Japan) and placed in a stereotaxic instrument (Narishige, Tokyo, Japan). A single 28 gauge stainless steel injection cannula (Eicom, Kyoto, Japan) was lowered into the right lateral ventricle (coordinates: −0.8 mm posterior to bregma, −1.5 mm lateral to midline, and −4.6 mm ventral to the skull surface) (Paxinos et al., 1985). The rats then received an acute i.c.v. injection of Accell siRNA (5 μg/rat) in 5 μL of Accell siRNA delivery media (Accell Control siRNA kit, Green, for rat; Thermo Scientific Dharmacon, Rockford, IL) at a rate of 0.5 μL/min using a microinfusion pump (type ESP-32, Eicom Corporation, Kyoto, Japan) and a 10 μL microsyringe (Hamilton Company, Tokyo, Japan). After the infusion was complete, the cannula was left in place for 5 min, then removed at a rate of 1 mm/min.

2.3. Histological analysis

Rats were deeply anesthetized with pentobarbital (70 mg/kg, i.p.) and perfused transcardially with 4% paraformaldehyde in 0.1 M phosphate-buffered saline (PBS; pH 7.4) on day 2, 4, or 7 post-siRNA injection. The brains were removed and postfixed in 4% paraformaldehyde in PBS at 4 °C overnight, stored in 30% sucrose in PBS at 4 °C for 2–3 days, and frozen at −80 °C until sectioning. The frozen tissue was cut on a cryostat into 15-μM coronal sections. Sections were taken through the following brain regions, relative to bregma (Paxinos et al., 1985): cortex and striatum (+2.16 to 0 mm), hippocampus (−2.28 to −3.96 mm), midbrain (−4.92 to −6.24 mm), and cerebellum (−9.24 to −9.96 mm).

2.3.1. Semi-quantification of FAM-labeled cells

To count cells incorporating FAM-labeled siRNA, brain sections were incubated for 10 min with 4′,6-diamidino-2-phenylindole (DAPI; 1 μg/mL; Dojindo, Kumamoto, Japan) to visualize all cells in the area of interest. Square images (5 × 5 mm) were captured by confocal microscopy (C1si-TE2000-E; Nikon, Tokyo, Japan). The raw images first were grayed, then were made binary using the Scion image software package (version 4.0.3., Scion cooperation, Fredrick, MD). The images were analyzed in two ways to detect the efficiency of siRNA incorporation into cells. First, the number of FAM-labeled cells among at least 500 total cells in the square image were counted manually. Second, the number of binary FAM-derived pixels in the square images were measured automatically. For each approach, three different sections were evaluated in each experimental group.

2.3.2. Identification of the types of cells labeled by FAM

Brain sections were treated with 0.3% Triton-X 100 in PBS three times for 5 min each, then were incubated with 10% goat serum in PBS for 30 min at room temperature to block nonspecific binding, and finally were incubated overnight at 4 °C with one of the following antibodies: mouse monoclonal anti-NeuN (1:1000; Millipore Japan, Tokyo, Japan), mouse monoclonal anti-glial fibrillary acidic protein (GFAP; 1:500; DAKO, Glostrup, Denmark), rabbit polyclonal anti-ionized calcium binding adaptor molecule-1 (Iba1; 1:500; WAKO pure chemicals, Osaka, Japan), or Fluoro 555-conjugated mouse monoclonal anti-2′3′ cyclic nucleotide 3′ phosphodiesterase (CNP; 1:200; Sigma–Aldrich, St. Louis, MO). The sections then were washed three times in PBS before being treated with Alexa 568-conjugated anti-mouse (for NeuN and GFAP) or anti-rabbit (for Iba1) IgG antibody (1:1000; Invitrogen, Carlsbad, CA) for 1 h. Cells double-labeled with FAM and a marker protein (NeuN, GFAP, Iba1, or CNP) were counted manually. Three different sections were evaluated in each experimental group.

2.3.3. Immunohistochemistry for cyclophilin-B and GAPDH

Brain sections were incubated with 10% goat serum in PBS for 30 min at room temperature to block nonspecific binding. For cyclophilin-B staining, the sections were incubated overnight at 4% with rabbit polyclonal anti-cyclophilin-B (1:1000; Abcam, Cambridge, UK). After three PBS washes, the sections were incubated in 0.3% hydrogen peroxide for 30 min, then were treated with a peroxidase-conjugated anti-rabbit IgG antibody (Histofine Simplestain MAX PO, Nichirei, Tokyo, Japan) for 1 h. The signal was visualized using a 3,3-diaminobenzidine (DAB) substrate kit (Vector Laboratories, Burlingame, CA). For staining of GAPDH, brain sections were pretreated in a microwave in 10 mM citrate buffer (pH 6.0) for 10 min, and incubated with 0.3% Triton-X 100 in PBS three times for 5 min each. The sections were incubated with 10% goat serum in PBS for 30 min at room temperature to block nonspecific binding, and finally were incubated with mouse monoclonal anti-GAPDH antibody (1:500; Millipore Japan) for 3 days at room temperature. After three PBS washes, the sections were incubated with Alexa 488-conjugated anti-mouse IgG antibody

(1:1000, Invitrogen) for 1 h. For nuclear staining, the cells were labeled with DAPI (1 μg/mL) for 10 min.

2.4. Western blotting

Brain regions of interest were dissected, immediately frozen in liquid nitrogen, and stored at −80 °C prior to being homogenized on ice for 1–2 min with a glass-teflon homogenizer in a lysis buffer (50 mM Tris–HCl, pH 7.5; 150 mM NaCl; 1 mM EDTA; 0.5% Nonidet P-40; 100 μM sodium vanadate; 1 mM sodium fluoride; 1 mM phenylmethylsulfonyl fluoride) containing a protease inhibitor cocktail (Nakalai Tesque, Inc., Kyoto, Japan). The samples were centrifuged (15,000 × *g* at 4 °C for 10 min) and the clear supernatants were retained. The protein concentration of the supernatants was determined using the Bradford assay (Bio-Rad, Hercules, CA). Five micrograms of protein per sample were separated by gel elecrophoresis using a 5–20% sodium dodecyl sulfate-polyacrylamide gel (SDS–PAGE; DRC, Tokyo, Japan) and transferred to a nitrocellulose transfer membrane (BioRad). The membranes were incubated for 1 h with Blocking-One (Nakalai tesque) in PBS containing 0.05% Tween-20 and 0.02% NaN_3 (PBST) to block nonspecific binding. The membranes were incubated overnight at 4 °C with anti-cyclophilin-B (1:2000) or anti-GAPDH (1:300), together with a mouse monoclonal anti-β-actin antibody (1:5000; Sigma–Aldrich, St. Louis, MO), in 10% Blocking-One/PBST buffer. Subsequently the membranes were incubated for 1 h at room temperature in a peroxidase-conjugated affinity-purified secondary antibody (Zymed Laboratories Inc., South San Francisco, CA). Detection was performed using ECL plus (GE Healthcare, Waukesha, WI). Band intensities were quantified with a LAS-3000 image analyzer (Fujifilm, Kanagawa, Japan).

3. Results

3.1. Delivery of Accell siRNA to brain by i.c.v. injection

To address whether Accell siRNA is effective in the adult rat brain, we injected Accell FAM-labeled control siRNA (5 μg/rat) i.c.v. as shown in Fig. 1A. The optimal concentration of siRNA was determined through preliminary experiments and is in accordance with published studies (Thakker et al., 2004, 2005). To investigate the time course of siRNA incorporation, we analyzed a cortical region (layer V; indicated by the green inset in Fig. 1A) in rats sacrificed 2, 4, or 7 days post-siRNA injection, using a confocal microscope. We were able to detect many fluorescent cells in this region (Fig. 1B). The incorporation efficiency of the siRNA was 21.4 ± 1.9% at day 2, 22.6 ± 3.6% at day 4, and 22.5 ± 3.1% at day 7. At days 2 and 4, the fluorescence was found in the cytoplasm, axonal structures, and dendritic neurites. At day 7, the fluorescence was concentrated almost entirely in the cytoplasm. Although FAM-labeled cells were detected consistently at all time points, the amount of incorporated FAM had decreased significantly by day 7 (Fig. 1C). Therefore, in subsequent experiments, we restricted our analysis to samples obtained at day 4 post-siRNA injection. We did not choose to examine day 2 because the reduction of target protein expression may not yet have been complete at this early time point. Additionally,

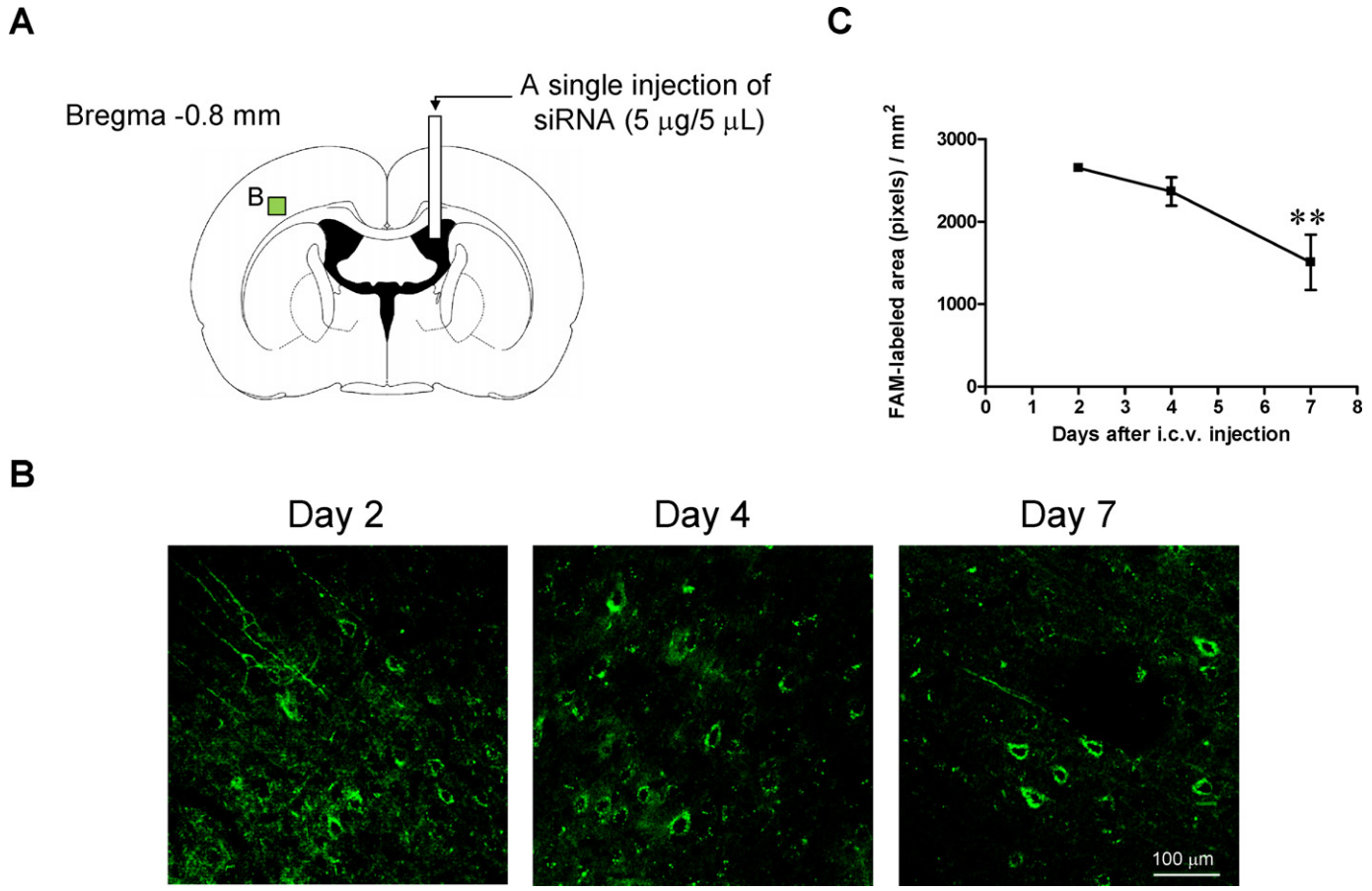

Fig. 1. Time course of siRNA incorporation following a single i.c.v. injection of Accell FAM-labeled control siRNA into the adult rat brain. (A) Schematic depicting the i.c.v. injection site and the cortical region of interest in analyses of siRNA incorporation (green inset). (B) Fluorescent images of Accell FAM-labeled control siRNA (green) in the cortical region of interest at days 2, 4, and 7 post-siRNA injection. (C) Semi-quantification of FAM labeling, defined as the FAM-labeled area (pixels)/mm². Shown is the mean ± standard deviation (SD) labeling across three brain sections at each time point. $^{**}p < 0.01$ vs. day 2, Dunnett's test.

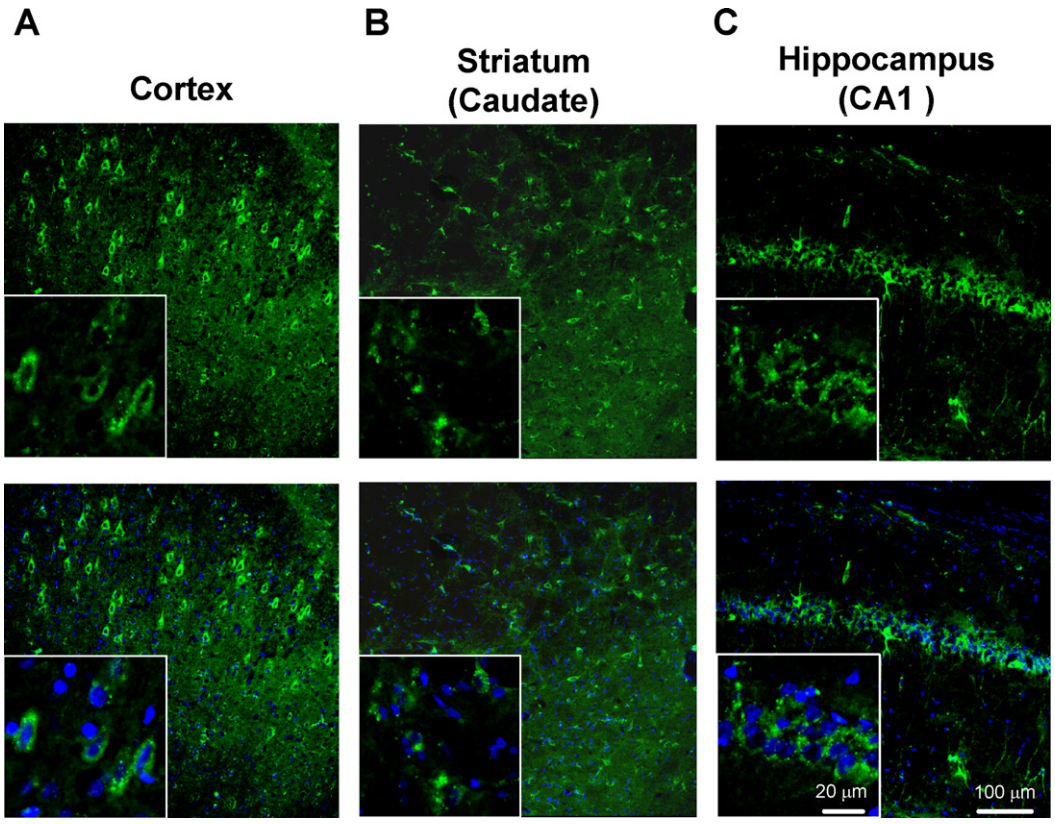

Fig. 2. Incorporation of Accell FAM-labeled control siRNA in cortical, striatal, and hippocampal neurons. The upper panels depict fluorescently labeled cells (green) in cortex (A), striatum (B), and hippocampus (C) into which Accell FAM-labeled control siRNA has been incorporated. In the lower panels, these images are merged with images of the same sections stained with DAPI, a nuclear stain (blue).

by day 7, it is possible that siRNA-associated side effects, including immune responses and/or unintended off-targeting effects, may have been evident.

3.2. Distribution of Accell siRNA in brain

Next, we examined the incorporation of Accell FAM-labeled control siRNA in various forebrain regions (Fig. 2). The strongest fluorescence was detected in the cortex (layers III and VI; Fig. 2A), the caudate subregion of the striatum (Fig. 2B), and hippocampal CA1 subregion pyramidal cells (Fig. 2C). We detected weaker fluorescence in layers I and II of cortex, the putamen subregion of the striatum, hippocampal CA3 subregion pyramidal cells, the thalamus, and the hypothalamus (data not shown). We also examined incorporation of Accell FAM-labeled control siRNA in the midbrain and cerebellum, and confirmed its presence in these regions as well (Fig. 3). The strongest fluorescence was detected in the substantia nigra (Fig. 3A) and in the molecular, granular, and medullary layers of the cerebellum (Fig. 3B). Particularly extensive incorporation was noted in the dopaminergic cells of the substantia nigra pars compacta and the Purkinje cells lying between the granular and medullary layers of the cerebellum. Altogether, these findings indicate that i.c.v. injection of Accell siRNA is a potent *in vivo* delivery system that is capable of inducing siRNA incorporation in various cell types in diverse brain regions.

3.3. Identification of the types of cells incorporated Accell siRNA

To further identify the types of cells into which Accell FAM-labeled control siRNA was incorporated, we used standard immunohistochemical procedures to stain for NeuN (a neuronal marker), GFAP (a marker of astrocytes), Iba1 (a marker of microglia),

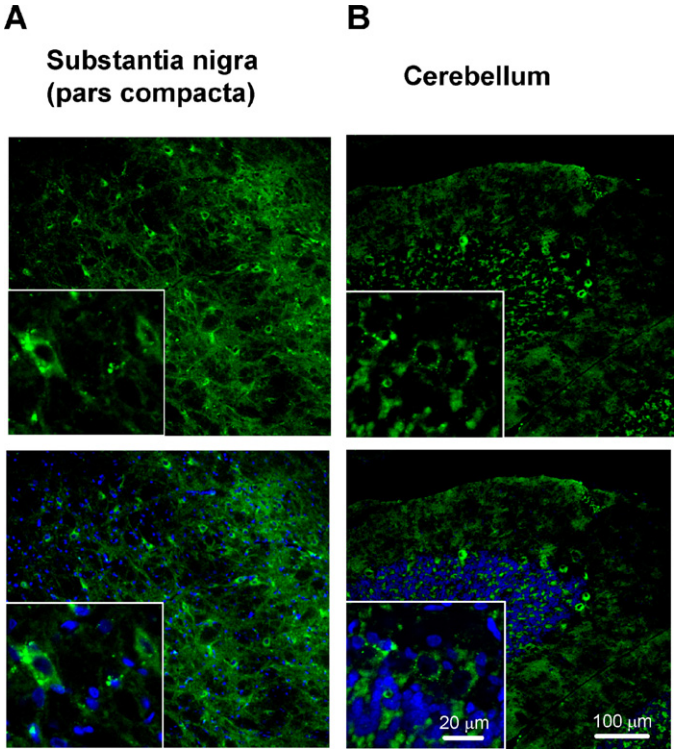

Fig. 3. Incorporation of Accell FAM-labeled control siRNA of the substantia nigra and cerebellum. The upper panels depict fluorescently labeled cells (green) in the substantia nigra pars compacta (A) and cerebellum (B) into which Accell FAM-labeled control siRNA has been incorporated. In the lower panels, these images are merged with images of the same sections stained with DAPI, a nuclear stain (blue).

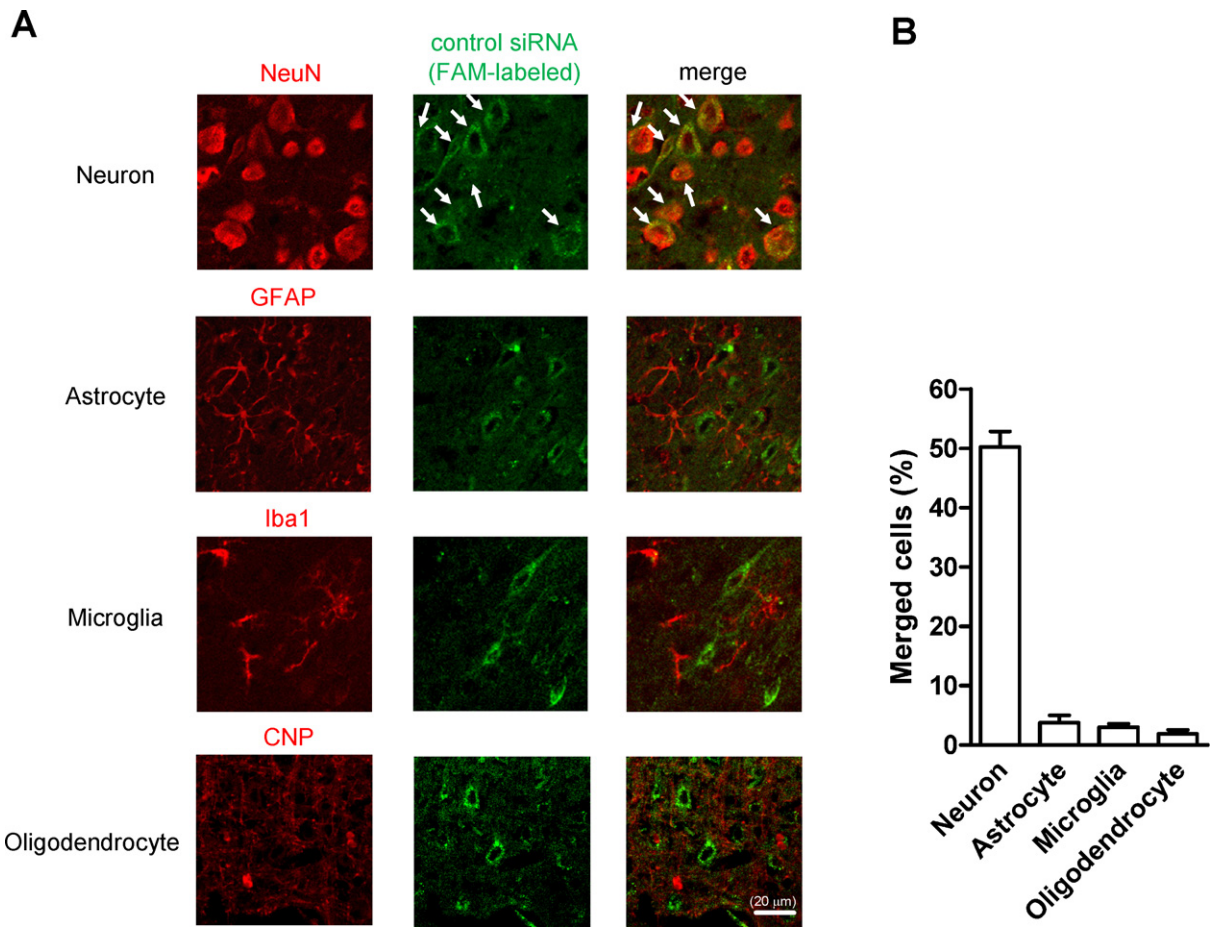

Fig. 4. Incorporation of Accell FAM-labeled control siRNA into neurons, astrocytes, and microglia. (A) The left panels depict immunohistochemical labeling (red) of NeuN (a neuronal marker), GFAP (a marker of astrocytes), Iba1 (a marker of microglia), and CNP (a marker of oligodendrocytes) in a cortical region of interest. The central panels show fluorescently labeled cells (green) into which Accell FAM-labeled control siRNA has been incorporated, in the same brain sections. In the right panels these two images are merged, showing co-labeling of FAM and cell type-specific markers. Arrows indicate cells incorporating Accell FAM-labeled control siRNA (B) Incorporation efficiency of Accell FAM-labeled control siRNA in neurons, astrocytes, microglia, and oligodendrocytes. Shown is the mean ± standard deviation (SD) percentage of double-labeled cells across three brain sections for each cell type-specific marker.

and CNP (a marker of oligodendrocyte) in cortical regions of brain sections from siRNA-injected rats (Fig. 4). Co-expression of FAM and NeuN was seen frequently (47.1 ± 3.9% of NeuN+ cells were also FAM +), whereas co-expression of FAM and GFAP was rare (2.9 ± 2.0% of GFAP+ cells were also FAM+) as was co-expression of FAM and Iba1 (2.8 ± 1.0% of Iba1+ cells were also FAM+) or co-expression of FAM and CNP (1.8 ± 1.4% of CNP+ cells were also FAM+). Of the FAM+ cells we observed, 97.1 ± 1.2% were neurons as indicated by NeuN staining. Together these results suggest that Accell siRNA enables neuron-specific gene silencing and protein knockdown.

3.4. Protein knockdowns of cyclophilin-B and GAPDH

Lastly, we examined whether i.c.v. injection of Accell siRNAs targeting specific genes would suppress the associated protein levels selectively. In these experiments we targeted cyclophilin-B, which is relatively abundant in neurons (Lane-Guermonprez et al., 2005), and GAPDH, a well-known reference protein in gene silencing experiments. Immunohistological analysis revealed that the expression of cyclophilin-B was decreased in cortex, the caudate subregion of striatum, and the CA1 subregion of hippocampus following a single i.c.v. injection of Accell rat cyclophilin-B siRNA, as compared to that seen following an injection Accell control siRNA (Fig. 5A). Cyclophilin-B knockdown was confirmed by Western blotting (Fig. 5B and C), which indicated that the decrease in expression was roughly 38–61%. We also used Western blotting to assess the time course of the cyclophilin-B knockdown (Supplementary Information) and found that it was similar to that seen in our earlier analyses of Accell FAM-labeled control siRNA incorporation (Fig. 1B and C). Similar effects on cyclophilin-B protein expression were observed in posterior brain regions including midbrain and cerebellum (Fig. 6). Following a single i.c.v. injection of Accell rat GAPDH siRNA, we observed effects on GAPDH expression in forebrain and posterior brain regions analogous to those seen with cyclophilin-B (Fig. 7). GAPDH knockdown in each brain region was roughly 23–34% (Fig. 7B and C) and the efficacy was relatively weak compared to that of cyclophilin-B, probably because the endogenous levels of GAPDH are very abundant in almost all of mammalian tissues.

4. Discussion

We have shown that a single i.c.v. injection of Accell siRNA into the adult rat brain leads to siRNA incorporation (Figs. 1–3) and knockdown of cyclophilin-B (Figs. 5 and 6; Supplementary Information) and GAPDH (Fig. 7) in neurons, not glia (Fig. 4). To our knowledge, ours is the first study to demonstrate successful *in vivo*, intra-CNS delivery of Accell siRNA.

Although we observed widespread incorporation of siRNA in diverse brain regions, we also found that certain cell types were resistant to siRNA incorporation. These include the granule cells of

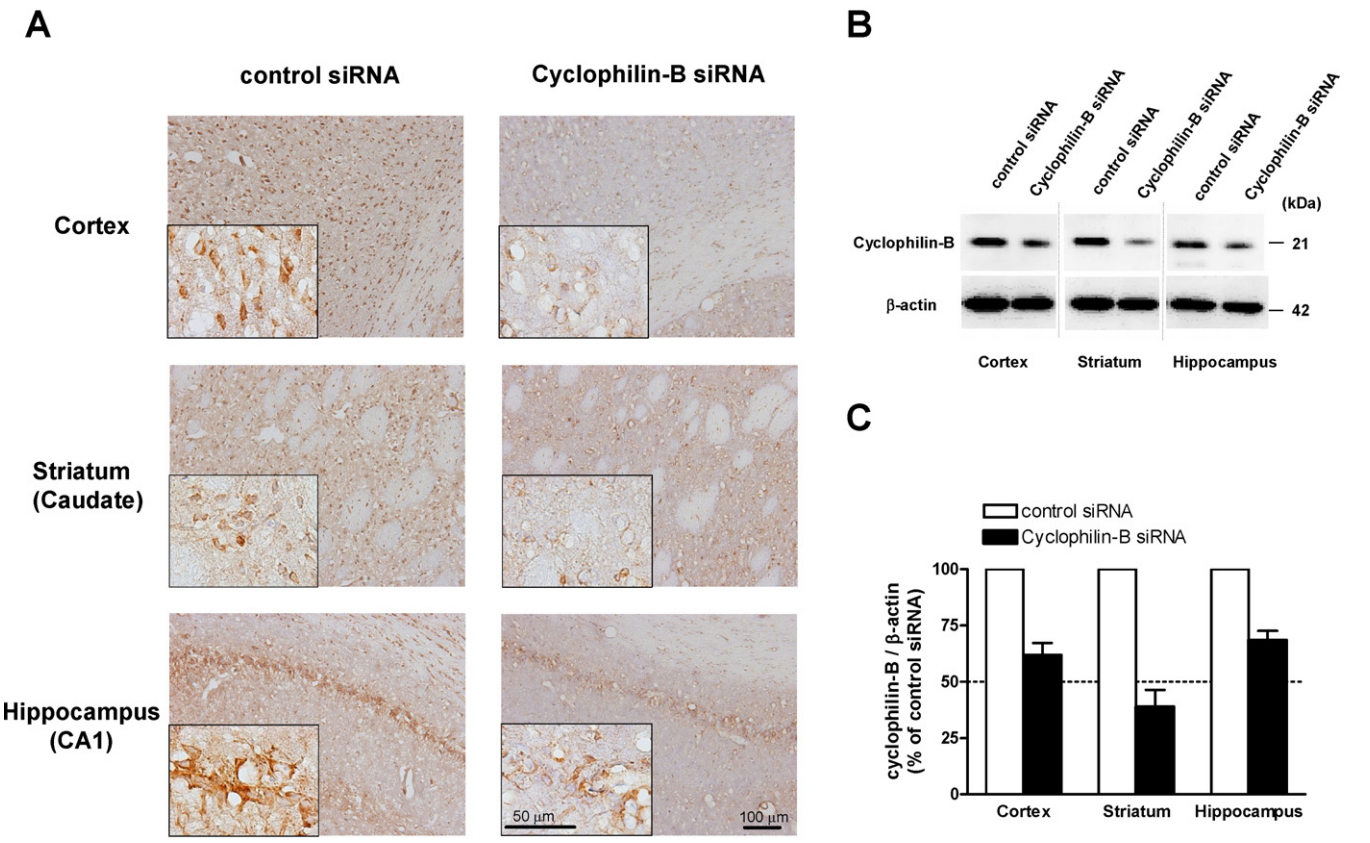

Fig. 5. Cyclophilin-B protein expression in cortex, striatum, and hippocampus following a single i.c.v. injection of Accell rat control siRNA or Accell rat cyclophilin-B siRNA. (A) Immunohistochemical staining for cyclophilin-B in cortex, striatum, and hippocampus in rat brains injected i.c.v. with Accell control siRNA (left panels) or Accell rat cyclophilin-B siRNA (right panels). Magnifications of selected portions of these images are shown in the insets. (B) Western blots depicting cyclophilin-B and β-actin expression in cortex, striatum, and hippocampus in rat brains injected i.c.v. with Accell control siRNA or Accell rat cyclophilin-B siRNA. (C) Semi-quantification of the band intensities in (B). For each sample, we calculated the ratio of the cyclophilin-B band intensity (quantified in arbitrary units) relative to the β-actin band intensity. We then expressed the ratio in the cyclophilin-B siRNA group as a percentage of the ratio in the control siRNA group. Shown is the mean ± standard deviation (SD) percentage ratio in each group across three brain sections for each brain region.

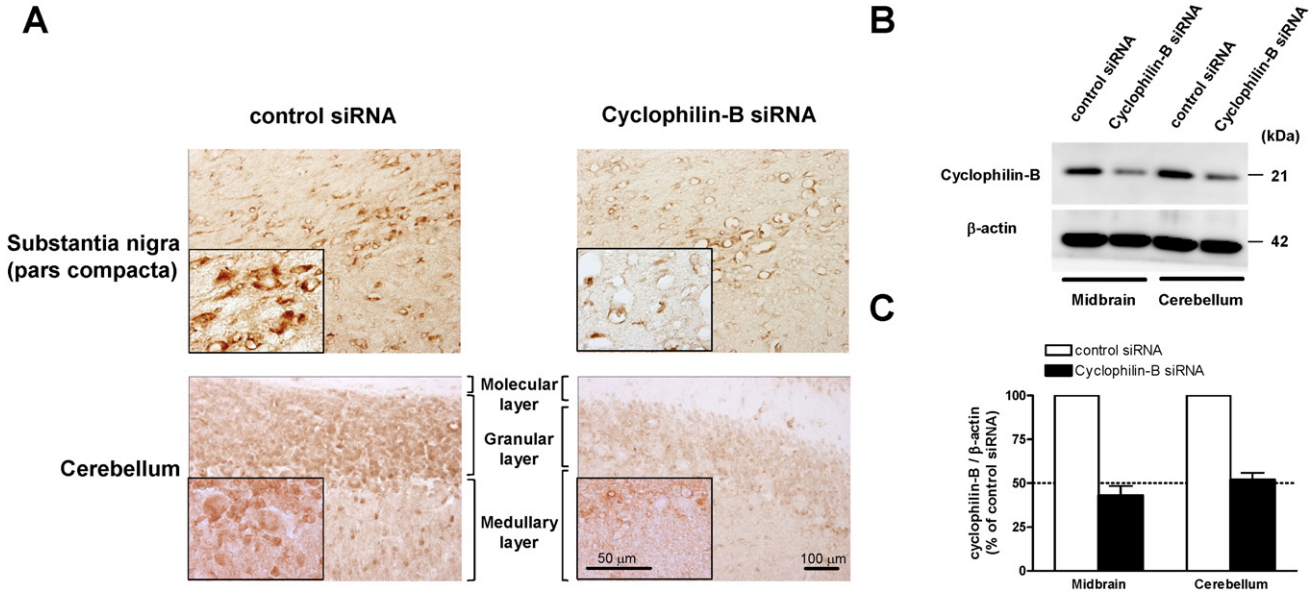

Fig. 6. Cyclophilin-B protein expression in substantia nigra and cerebellum following a single i.c.v. injection of Accell rat control siRNA or Accell rat cyclophilin-B siRNA. (A) Immunohistochemical staining for cyclophilin-B in substantia nigra and cerebellum in rat brains injected i.c.v. with Accell control siRNA (left panels) or Accell rat cyclophilin-B siRNA (right panels). Magnifications of selected portions of these images are shown in the insets. (B) Western blots depicting cyclophilin-B and β-actin expression in midbrain and cerebellum in rat brains injected i.c.v. with Accell control siRNA or Accell rat cyclophilin-B siRNA. (C) Semi-quantification of the band intensities in (B). For each sample, we calculated the ratio of the cyclophilin-B band intensity (quantified in arbitrary units) relative to the β-actin band intensity. We expressed the ratio in the cyclophilin-B siRNA group as a percentage of the ratio in the control siRNA group. Shown is the mean ± standard deviation (SD) percentage ratio in each group across three brain sections for each brain region.

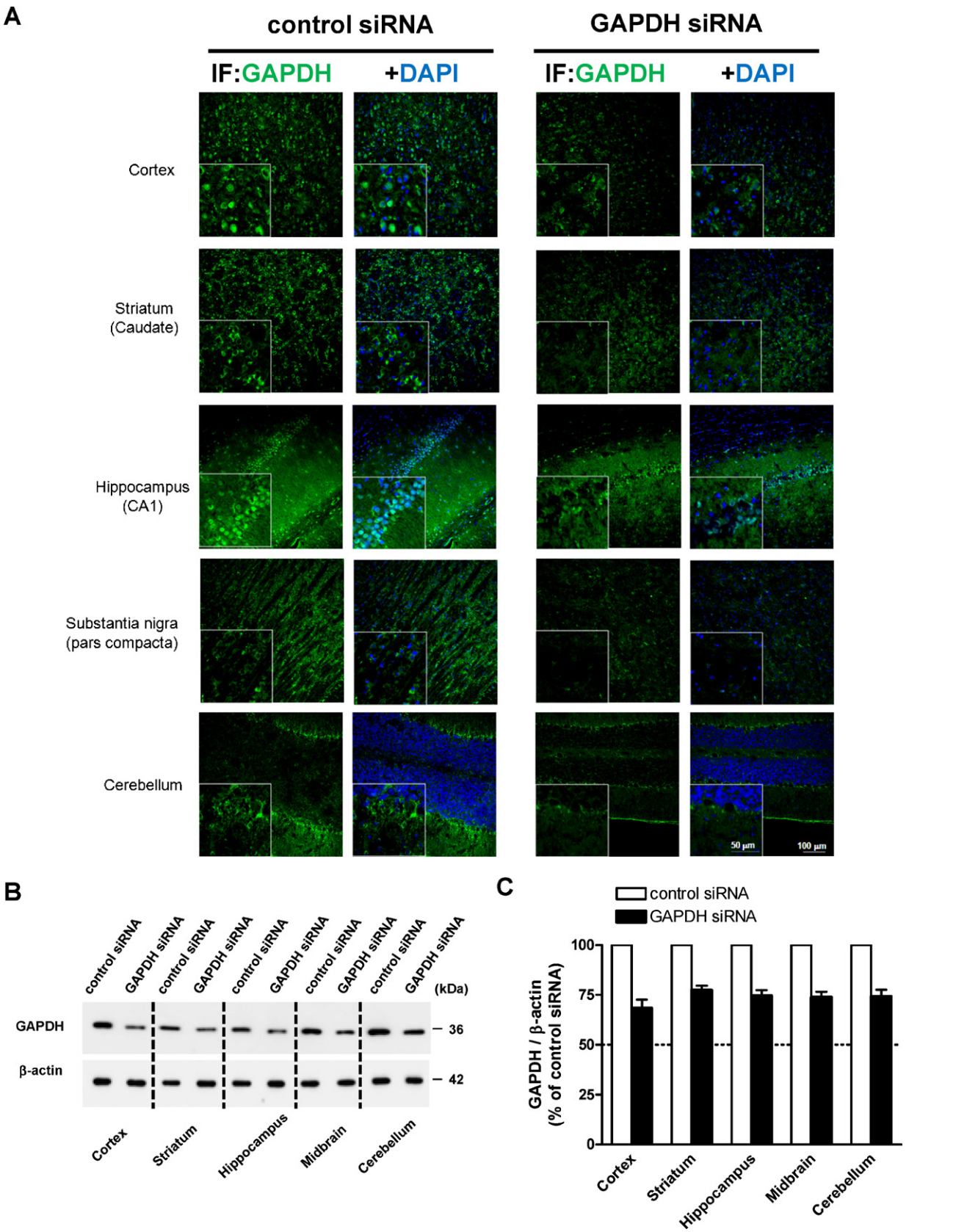

Fig. 7. GAPDH protein expression in cortex, striatum, hippocampus, substantia nigra, and cerebellum following a single i.c.v. injection of Accell rat control siRNA or Accell rat GAPDH siRNA. (A) Immunohistochemical staining for GAPDH (green) and merged images showing GAPDH staining (green) and DAPI staining (blue) in cortex, the caudate region of striatum, the CA1 region of hippocampus, substantia nigra pars compacta, and cerebellum in rat brains injected i.c.v. with Accell control siRNA (left panels) or Accell rat GAPDH siRNA (right panels). (B) Western blots depicting GAPDH and β-actin expression in cortex, striatum, hippocampus, midbrain, and cerebellum in rat brains injected i.c.v. with Accell control siRNA or Accell rat GAPDH siRNA. (C) Semi-quantification of the band intensities in (B). For each sample, we calculated the ratio of the GAPDH band intensity (quantified in arbitrary units) relative to the β-actin band intensity. We expressed the ratio in the GAPDH siRNA group as a percentage of the ratio in the control siRNA group. Shown is the mean ± standard deviation (SD) percentage ratio in each group across three brain sections for each brain region.

the dentate gyrus (data not shown) and glia (astrocytes, microglia, and oligodendrocytes; Fig. 4). The dentate gyrus is one of the few mammalian brain regions that continues to generate new neurons through adulthood (Mathews et al., 2010), and astrocytes, microglia, and oligodendrocytes are proliferating cells. Thus, we hypothesize that Accell siRNA incorporation may be selective to mature cells rather than differentiating ones, at least in the CNS. Further study of the mechanisms of Accell siRNA incorporation in neurons is needed.

There are several advantages of *in vivo* over *in vitro* studies of the effects of gene silencing and protein knockdown (Shim and Kwon, 2010). One of these is that *in vivo* studies allow for the identification of adverse effects, such as siRNA-induced immune responses that would not be evident *in vitro*. In the present study Accell siRNA was not associated with swelling or gliosis (proliferation of astrocytes or appearance of ameboid types of microglia), suggesting that toxicity and neuroinflammation were absent. Hence, the rapid and convenient method of siRNA delivery that we have employed is relatively benign, underlining its potential experimental utility *in vivo*.

The novel protocol we describe is likely to be useful not only in experimental investigations of neuropathophysiological mechanisms, but also in the clinical application of RNAi in the treatment of neurodegenerative and neuropsychiatric disorders. Therefore, we suggest that the present study will be of interest to a diverse audience, including both basic scientists interested in medical biotechnology, especially *in vivo,* intra-CNS delivery of siRNA in animal models, and clinical scientists searching for novel therapeutic strategies.

5. Conclusion

In the present study, we have developed a new procedure involving a single i.c.v. injection of Accell siRNA into the adult rat brain to induce neuron-specific protein knockdown in the CNS. The method is simple, produces rapid effects, lends itself well to experimental investigations of neural pathophysiology, and provides a hint to potential clinical utility as a tool in the treatment of neurodegenerative and neuropsychiatric disorders.

Acknowledgements

We thank Dr. Akira Sawa (Johns Hopkins University School of Medicine) and Miyuu Tanaka (Osaka Prefecture University) for helpful discussion. This work was supported in part by a Grant-in-Aid (22580339) from the Japan Society for the Promotion of Science (to H.N.).

Appendix A. Supplementary data

Supplementary data associated with this article can be found, in the online version, at doi:10.1016/j.jbiotec.2011.10.003.

References

Akhtar, S., Benter, I.F., 2007. Nonviral delivery of synthetic siRNAs in vivo. J. Clin. Invest. 117, 3623–3632.
Alvarez-Erviti, L., Seow, Y., Yin, H., Betts, C., Lakhal, S., Wood, M.J., 2011. Delivery of siRNA to the mouse brain by systemic injection of targeted exosomes. Nat. Biotechnol. 29, 341–345.
Baskin, L., Urschel, S., Eiberger, B., 2008. A novel ex-vivo application of RNAi for neuroscience. Biotechniques 45, 338–339.
Bonifazi, P., D'Angelo, C., Zagarella, S., Zelante, T., Bozza, S., De Luca, A., Giovannini, G., Moretti, S., Iannitti, R.G., Fallarino, F., Carvalho, A., Cunha, C., Bistoni, F., Romani, L., 2010. Intranasally delivered siRNA targeting PI3K/Akt/mTOR inflammatory pathways protects from aspergillosis. Mucosal Immunol. 3, 193–205.
Chen, C., Hu, Q., Yan, J., Yang, X., Shi, X., Lei, J., Chen, L., Huang, H., Han, J., Zhang, J.H., Zhou, C., 2009. Early inhibition of HIF-1alpha with small interfering RNA reduces ischemic-reperfused brain injury in rats. Neurobiol. Dis. 33, 509–517.
Chen, S.H., Zhaori, G., 2011. Potential clinical applications of siRNA technique: benefits and limitations. Eur. J. Clin. Invest. 41, 221–232.
de Fougerolles, A., Vornlocher, H.P., Maraganore, J., Lieberman, J., 2007. Interfering with disease: a progress report on siRNA-based therapeutics. Nat. Rev. Drug Discov. 6, 443–453.
Difeo, A., Huang, F., Sangodkar, J., Terzo, E.A., Leake, D., Narla, G., Martignetti, J.A., 2009. KLF6-SV1 is a novel antiapoptotic protein that targets the BH3-only protein NOXA for degradation and whose inhibition extends survival in an ovarian cancer model. Cancer Res. 69, 4733–4741.
Dolga, A.M., Granic, I., Blank, T., Knaus, H.G., Spiess, J., Luiten, P.G., Eisel, U.L., Nijholt, I.M., 2008. TNF-alpha-mediates neuroprotection against glutamate-induced excitotoxicity via NF-kappaB-dependent up-regulation of K2.2 channels. J. Neurochem. 107, 1158–1167.
Dreses-Werringloer, U., Lambert, J.C., Vingtdeux, V., Zhao, H., Vais, H., Siebert, A., Jain, A., Koppel, J., Rovelet-Lecrux, A., Hannequin, D., Pasquier, F., Galimberti, D., Scarpini, E., Mann, D., Lendon, C., Campion, D., Amouyel, P., Davies, P., Foskett, J.K., Campagne, F., Marambaud, P., 2008. A polymorphism in CALHM1 influences Ca2+ homeostasis, Abeta levels, and Alzheimer's disease risk. Cell 133, 1149–1161.
Dreyer, J.L., 2011. Lentiviral vector-mediated gene transfer and RNA silencing technology in neuronal dysfunctions. Mol. Biotechnol. 47, 169–187.
Elbashir, S.M., Harborth, J., Lendeckel, W., Yalcin, A., Weber, K., Tuschl, T., 2001. Duplexes of 21-nucleotide RNAs mediate RNA interference in cultured mammalian cells. Nature 411, 494–498.
Hu, Q., Chen, C., Yan, J., Yang, X., Shi, X., Zhao, J., Lei, J., Yang, L., Wang, K., Chen, L., Huang, H., Han, J., Zhang, J.H., Zhou, C., 2009. Therapeutic application of gene silencing MMP-9 in a middle cerebral artery occlusion-induced focal ischemia rat model. Exp. Neurol. 216, 35–46.
Jean, A., Conductier, G., Manrique, C., Bouras, C., Berta, P., Hen, R., Charnay, Y., Bockaert, J., Compan, V., 2007. Anorexia induced by activation of serotonin 5-HT4 receptors is mediated by increases in CART in the nucleus accumbens. Proc. Natl. Acad. Sci. U.S.A. 104, 16335–16340.
Kumar, P., Wu, H., McBride, J.L., Jung, K.E., Kim, M.H., Davidson, B.L., Lee, S.K., Shankar, P., Manjunath, N., 2007. Transvascular delivery of small interfering RNA to the central nervous system. Nature 448, 39–43.
Lane-Guermonprez, L., Morot-Gaudry-Talarmain, Y., Meunier, F.M., O'Regan, S., Onofri, F., Le Caer, J.P., Benfenati, F., 2005. Synapsin associates with cyclophilin B in an ATP- and cyclosporin A-dependent manner. J. Neurochem. 93, 1401–1411.
Lingor, P., Koeberle, P., Kugler, S., Bahr, M., 2005. Down-regulation of apoptosis mediators by RNAi inhibits axotomy-induced retinal ganglion cell death in vivo. Brain 128, 550–558.
Makimura, H., Mizuno, T.M., Mastaitis, J.W., Agami, R., Mobbs, C.V., 2002. Reducing hypothalamic AGRP by RNA interference increases metabolic rate and decreases body weight without influencing food intake. BMC Neurosci. 3, 18.
Manrique, C., Compan, V., Rosselet, C., Duflo, S.G., 2009. Specific knock-down of GAD67 in the striatum using naked small interfering RNAs. J. Biotechnol. 142, 185–192.
Mathews, E.A., Morgenstern, N.A., Piatti, V.C., Zhao, C., Jessberger, S., Schinder, A.F., Gage, F.H., 2010. A distinctive layering pattern of mouse dentate granule cells is generated by developmental and adult neurogenesis. J. Comp. Neurol. 518, 4479–4490.
Paxinos, G., Watson, C., Pennisi, M., Topple, A., 1985. Bregma, lambda and the interaural midpoint in stereotaxic surgery with rats of different sex, strain and weight. J. Neurosci. Methods 13, 139–143.
Pulford, B., Reim, N., Bell, A., Veatch, J., Forster, G., Bender, H., Meyerett, C., Hafeman, S., Michel, B., Johnson, T., Wyckoff, A.C., Miele, G., Julius, C., Kranich, J., Schenkel, A., Dow, S., Zabel, M.D., 2010. Liposome–siRNA–peptide complexes cross the blood–brain barrier and significantly decrease PrP on neuronal cells and PrP in infected cell cultures. PLoS One 5, e11085.
Sebeo, J., Hsiao, K., Bozdagi, O., Dumitriu, D., Ge, Y., Zhou, Q., Benson, D.L., 2009. Requirement for protein synthesis at developing synapses. J. Neurosci. 29, 9778–9793.
Shim, M.S., Kwon, Y.J., 2010. Efficient and targeted delivery of siRNA in vivo. FEBS J. 277, 4814–4827.
Suzuki, S., Yokoyama, U., Abe, T., Kiyonari, H., Yamashita, N., Kato, Y., Kurotani, R., Sato, M., Okumura, S., Ishikawa, Y., 2010. Differential roles of Epac in regulating cell death in neuronal and myocardial cells. J. Biol. Chem. 285, 24248–24259.
Thakker, D.R., Natt, F., Husken, D., Maier, R., Muller, M., van der Putten, H., Hoyer, D., Cryan, J.F., 2004. Neurochemical and behavioral consequences of widespread gene knockdown in the adult mouse brain by using nonviral RNA interference. Proc. Natl. Acad. Sci. U.S.A. 101, 17270–17275.
Thakker, D.R., Natt, F., Husken, D., van der Putten, H., Maier, R., Hoyer, D., Cryan, J.F., 2005. siRNA-mediated knockdown of the serotonin transporter in the adult mouse brain. Mol. Psychiatry 10 (782–789), 714.
Walton, S.P., Wu, M., Gredell, J.A., Chan, C., 2010. Designing highly active siRNAs for therapeutic applications. FEBS J. 277, 4806–4813.
Zhao, M.G., Toyoda, H., Lee, Y.S., Wu, L.J., Ko, S.W., Zhang, X.H., Jia, Y., Shum, F., Xu, H., Li, B.M., Kaang, B.K., Zhuo, M., 2005. Roles of NMDA NR2B subtype receptor in prefrontal long-term potentiation and contextual fear memory. Neuron 47, 859–872.
Zimmermann, T.S., Lee, A.C., Akinc, A., Bramlage, B., Bumcrot, D., Fedoruk, M.N., Harborth, J., Heyes, J.A., Jeffs, L.B., John, M., Judge, A.D., Lam, K., McClintock, K., Nechev, L.V., Palmer, L.R., Racie, T., Rohl, I., Seiffert, S., Shanmugam, S., Sood, V., Soutschek, J., Toudjarska, I., Wheat, A.J., Yaworski, E., Zedalis, W., Koteliansky, V., Manoharan, M., Vornlocher, H.P., MacLachlan, I., 2006. RNAi-mediated gene silencing in non-human primates. Nature 441, 111–114.